

IEEE VTS Motor Vehicles Challenge 2017 – Energy Management of a Fuel Cell/Battery Vehicle

Clément Dépature^{1,2,4}, Samir Jemeï^{3,4}, Loïc Boulon¹, Alain Bouscayrol^{2,4}, Neigel Marx^{3,4}, Simon Morando³, Ali Castaings^{2,4}

¹ Université du Québec à Trois-Rivières, GRÉI, Trois-Rivières, Canada

² University of Lille 1, L2EP, Lille, France

³ University of Bourgogne Franche-Comté, FCLAB (FR CNRS 3539), FEMTO-ST (UMR CNRS 6174), Belfort, France

⁴ French network on HEVs, MEGEVH, megevh.org, France

*Corresponding author: samir.jemei@univ-fcomte.fr; Loic.Boulon@uqtr.ca

Abstract — This paper proposes a challenge focused on the energy management of a Fuel Cell/Battery Vehicle. Both Academic and Professional teams are welcomed to participate in this challenge. The aim of this challenge is to develop a robust Energy Management Strategy to increase the energy sources' lifetime and to minimize the hydrogen consumption. In this way, the simulation model and control presented in this paper will be provided to the challenge participants (downloadable Matlab Simulink file). The top scoring participants will be distinguished and invited to present their results in a special session at the 2017 IEEE VPPC.

Keywords — Energetic Macroscopic Representation, Energy management, Fuel Cell, Hybrid Electric Vehicle

I. INTRODUCTION

The IEEE Vehicular Technology Society, the University of Quebec à Trois-Rivières, L2EP laboratory, FCLAB Research federation, FEMTO-ST Institute and the French network on HEVs (MEGEVH) launch the IEEE VTS Motor Vehicles Challenge 2017. The challenge focuses on the energy management of a Fuel Cell Vehicle. Both Academic (from University or College) and Professional teams are welcomed to participate in this challenge. The top scoring participants will be distinguished and invited to present their results in a special session at the 2017 IEEE VPPC.

Hybrid Electric Vehicles (HEVs) combine the benefits of different sources [1] [2]. They can be designed to meet different goals, such as reducing the fuel consumption. Nevertheless, the Energy Management Strategy (EMS) appears as a critical issue for HEVs [3]-[8]. Indeed, the EMS determines which power source has to be operated according to the mission profile and the technical specifications of the sources. In the considered architecture proposed for this challenge, a Proton Exchange Membrane Fuel Cell (PEMFC) system and a battery pack provide the power to the traction system [9], which is based on the commercial Tazzari Zero electric vehicle (Fig. 1) [10].

In the framework of this challenge, a complete vehicle model and the associated control is provided. The participants will have to design the energy management strategy. This

strategy could be design to minimize two important aspects: the fuel consumption and the energy source degradations.

Hydrogen (H₂) is a promising energy carrier. This fuel has a high specific energy of 33.3 kWh/kg and is perceived as “clean” because the H₂ combustion generates water. However, pure hydrogen is not naturally occurring. Its production methods are varied but require energy and are expensive [11].

Fuel Cells are well-known candidates for the next energy sources in HEVs but they are still facing some degradations [12] [13]. The main degradations are induced by the dynamical loads and also the numbers of start and stop events. For example, a PEMFC used in an automotive application is estimated to undergo over 1 200 start/stop cycles during its lifetime [14]. Thus, it is important to limit these cycles when designing the EMS. For batteries, the State-of-Charge (SoC) range should be limited to avoid premature degradations [15].

The aim of this challenge is to develop a robust Energy Management Strategy to:

- Minimize the fuel (hydrogen) consumption,
- Increase the power and energy sources' lifetime by (i) minimizing start/stop cycles of the PEMFC and (ii) limiting the batteries' state of charge.

In section II, the studied FC/Battery EV is presented. The organization of the EV model and its control are depicted using Energetic Macroscopic Representation (EMR) in section III. The energy management design specifications and the scoring procedure are finally described in section IV.



Fig. 1 Reference commercial electric vehicle for the traction

II. STUDIED FUEL CELL/BATTERY VEHICLE

The studied vehicle is a 698 kg (mass without passengers) heavy quadricycle equipped with a single ratio gearbox, a differential and two driven-wheels. The propulsion system is composed of a 15 kW induction machine fed by a voltage-source-inverter through a 80 V - 40 Ah Lithium Iron Phosphate (LiFePO4) battery pack (Fig. 2). The vehicle is limited at a maximum speed up to 85 km/h.

The Fuel Cell is a 16 kW, 40-60 V, PEMFC system; with a maximum current up to 400 A. A compressor ensures the supply of oxygen, and a carbon fiber/epoxy composite tank stores 5.5 kg of H₂ at 350 bar. The FC is connected to the vehicle traction sub-system thanks to a non-reversible boost chopper and a smoothing inductor (Fig. 2). The battery is directly connected to the traction sub-system. In this way, the main advantage of this topology is to limit the number of converter, and then the weight, the size and even the cost of the vehicle. The FC is assumed as an equivalent voltage source. The studied vehicle parameters are presented in Table 1.

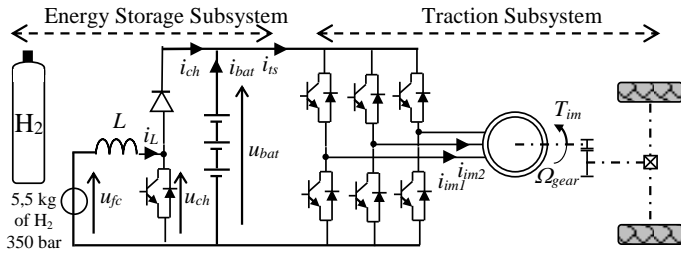


Fig. 2 Studied fuel cell/battery vehicle architecture

TABLE 1 FUEL CELL/BATTERY VEHICLE PARAMETERS

Fuel Cell	40-60 V, 16 kW
Smoothing inductors	5.5 mΩ, 0.25 mH
Battery	80 V, 40 Ah
Electric drive	15 kW
Vehicle mass	698 kg

III. MODELLING AND CONTROL OF THE RANGE EXTENDER FUEL CELL VEHICLE

The following simulation model and control will be provided to the challenge participants (downloadable Matlab Simulink™ file). All the numerical values of the parameters will be provided as an initialization file.

Energetic Macroscopic Representation (EMR) is a graphical description for the definition of control schemes of complex energetic systems [16] [17]. Different pictograms are then used (see Appendix). Green oval pictograms represent source elements, which can be energy generators and/or receptors; they are the terminals of the system. Orange rectangle pictograms with diagonal line represent accumulation elements, which store energy and impose state variables. Orange squares describe conversion of energy in the same domain without internal energy accumulation (mono-domain conversion). Orange circles are similar but the energy conversion is ensured between different physical

fields (multi-domain conversion). Overlapped orange pictograms describe coupling elements, which distribute energy (without energy accumulation). All elements are connected according to the action/reaction principle, and the scalar product of the action and reaction vectors yields the instantaneous power exchanged by the elements. Moreover, the accumulation elements impose inputs and outputs to other elements according to the physical causality principle (exclusive integral causality).

A control scheme can be directly defined from the EMR of the system using inversion rules. All control pictograms are depicted by blue parallelograms. An accumulation element is inverted using a closed-loop control. Any conversion element can be directly inverted without control loop. Coupling elements are inverted using distribution inputs in order to define the distribution of energy within the system. The inversion of the EMR of the system leads to a maximum control structure with a maximum of sensors and control operations. Simplifications and estimations can be performed in further steps. Finally a supervision level, called strategy, is used in order to define the local control references and the different distribution inputs.

A. Modelling

The FC is considered as a voltage source using its static polarization curve (quasi-static model experimentally validated) (Fig. 3. a). In addition, a static characteristic represents the H₂ mass flow versus current linear function that describes the FC system consumption (Fig. 3. b). In order to take into account the added on-board energy source, the State-of-Charge of the H₂ tank SoC_{H_2} is estimated from the relationship:

$$SoC_{H_2} = \frac{m_{H_2-init} - \int \dot{m}_{H_2}(i_{fc})}{m_{H_2-init}} \quad (1)$$

with m_{H_2-init} the initial mass of H₂ [g], \dot{m}_{H_2} the H₂ mass flow [g/s] and i_{fc} the FC current.

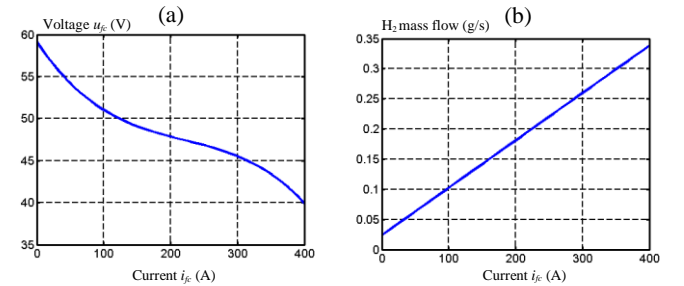


Fig. 3 (a) Fuel Cell polarization curve and (b) Fuel Cell consumption curve

The FC system is composed of the FC, a smoothing inductor (2) and a boost chopper (3) for its current control [18]. Other ancillaries (air supply system, cooling system, etc) are not explicitly modeled. Nevertheless, their energetic performances are included into the FC static characteristics.

$$L \frac{d}{dt} i_{fc} = u_{fc} - u_{hfc} - r_L i_{fc} \quad (2)$$

$$\begin{cases} u_{hfc} = m_{hfc} u_{bat} \\ i_{hfc} = m_{hfc} i_{fc} \eta_{hfc}^k \end{cases} \text{ with } k = \begin{cases} 1 & \text{if } P > 0 \\ -1 & \text{if } P < 0 \end{cases} \quad (3)$$

where L and r_L are the inductance and resistance of the smoothing inductor, m_{hfc} is the modulation ratio of the FC chopper and $\eta_{hfc}=95\%$ is the average efficiency of the chopper.

The battery is modeled using an open-circuit voltage u_0 with a series resistance R_s , and a parallel combination of resistance capacitance $R_c C_c$ (Fig. 4) [19] following (4).

$$i_{bat} = \frac{u_0 - R_s i_{bat} - u_{bat}}{R_c} + C_c \frac{d}{dt} (u_0 - R_s i_{bat} - u_{bat}) \quad (4)$$

where u_0 , R_s , R_c and C_c are estimated from experimental tests. The SoC of the battery SoC_{bat} is estimated from the initial SoC of the battery SoC_{init} , the battery capacity Q_{bat} and the battery current i_{bat} following the relationship (5):

$$SoC_{bat} = SoC_{init} - \frac{100}{3600 Q_{bat}} \int i_{bat} dt \quad (5)$$

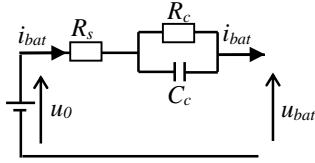


Fig. 4 Battery structural model

The parallel connection between the FC system, the battery and the traction system is modeled by the Kirchhoff's current law:

$$i_{bat} = i_{ts} - i_{hfc} \quad (6)$$

In order to simplify the study, a static model is considered for the traction subsystem, according to an efficiency map (Fig. 5). It includes the inverter associated with the traction machine, the wheels, the gearbox, the mechanical transmission and the control algorithm [20]. This model was experimentally validated and is relevant to address the problem of energy management's performance study. The traction system is directly controlled by a reference traction force $F_{trans-ref}$.

$$\begin{cases} F_{trans} = F_{trans-ref} \\ i_{ts} = \frac{F_{trans} v_{ev}}{u_{bat} (\eta_{tract})^k} \end{cases} \text{ with } k = \begin{cases} 1 & \text{if } P_{tract} > 0 \\ -1 & \text{if } P_{tract} < 0 \end{cases} \quad (7)$$

The mechanical brake generates a negative braking force F_b following the drive requirement. It is then added to the transmission force F_{trans} to obtain the total traction force F_{tract} :

$$F_{tract} = F_{trans} + F_b \quad (8)$$

The chassis is considered as an equivalent total mass M_{tot} (mass of the vehicle and the equivalent mass of the rotating

parts). The vehicle velocity v_{ev} is obtained by using Newton's second law of motion with the traction and resistive forces, F_{tract} and F_{res} :

$$M_{tot} \frac{d}{dt} v_{ev} = F_{tract} - F_{res} \quad (9)$$

$$F_{res} = f M_{tot} g + 0.5 \rho c_x A (v_{ev} + v_{wind})^2 + M_{tot} g \alpha \quad (10)$$

with f the rolling resistance coefficient, g the acceleration due to gravity, α the slope rate, c_x the air drag coefficient and A the frontal area of the vehicle.

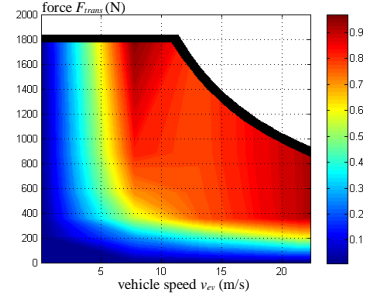


Fig. 5 Efficiency map η_{tract} of the traction subsystem

B. EMR and Deduced Control

The EMR of the studied vehicle is deduced (upper part of Fig. 6) from the relationships presented in section A. Each components are connected each other in respect with the interaction principle.

The FC system and the battery are considered as electrical sources and the vehicle environment and brake as mechanical sources. The traction system is considered as a multi-domain conversion element with the voltage u_{bat} and the velocity v_{ev} as inputs, the current i_{ts} and the force F_{trans} as outputs, and the reference force $F_{trans-ref}$ as a tuning input. The chopper is a mono-domain conversion element connected to the battery with a coupling element (parallel connection). The inductor and the chassis are accumulation elements; which lead to the current i_{fc} and the vehicle velocity v_{ev} as state variables.

The control scheme is deduced from the EMR, using inversion-based rules (lower part in Fig. 6) [16] [17]. All variables can be measured.

The Energy Storage Subsystem (ESS) objective is to control the FC current. From the EMR, a tuning path that links the tuning variable m_{hfc} to the variable i_{fc} to be controlled is deduced. This tuning path is then inverted to obtain a corresponding control path. The output energetic variable i_{fc} then became a reference control input i_{fc-ref} . The control structure is finally obtained by inversion of the EMR elements crossed by the defined tuning path. The inversion of the smoothing inductor model (2) yields the reference of the chopper voltage, $u_{hfc-ref}$. The inversion of the chopper model (3) yields the reference of the modulation ratio.

$$u_{hfc-ref} = -C_i(t) (i_{fc-ref} - i_{fc-meas}) + u_{fc-meas} \quad (11)$$

$$m_{hfc} = \frac{u_{hfc-ref}}{u_{bat-meas}} \quad (12)$$

where $C_i(t)$ is a PI controller. In addition, a low frequency filtering of 15 mHz and a ramp load limitation of 6 to 20 A/sec is respected depending on the FC power for the fuel cell current i_{fc-ref} generation. This reduces stack faults and degradation [12].

To ensure the desired vehicle velocity, the tuning variable $F_{trans-ref}$ is linked to the variable to be controlled (v_{ev}). From the desired vehicle speed v_{ev-ref} , the measured vehicle velocity v_{ev} and the estimated environment force F_{res} , the reference transmission force $F_{trans-ref}$ is provided from (9) by using:

$$F_{trans-ref} = C_v(t)(v_{ev-ref} - v_{ev-meas}) + F_{res-meas} \quad (13)$$

with $C_v(t)$ is a PI controller. Furthermore, a traction force and power limitations of 2000 N / 15 kW are respected to limit the current draw which can degrade the ESS or the traction subsystem. This control saturation is finally taken into account by the speed controller by using an anti-windup control loop [21] [22].

The mechanical coupling, which adds the brakes and the mechanical transmission forces (8), is then inverted using a distribution input k_D :

$$\begin{cases} F_{trans-ref} = k_D F_{tract-ref} \\ F_{b-ref} = (1 - k_D) F_{tract-ref} \end{cases} \quad (14)$$

Two strategy-level inputs need to be defined by the participants (strategy block of Fig. 6). First, the mechanical and electrical distribution of the braking force must be realized from the braking distribution parameter k_D following (14). As only the front wheels are connected to the traction machine, k_D must be limited to the maximum value of 0.5 for the braking phases. Finally, the FC current reference value i_{fc-ref} must also be determined according to several rules that will be defined in the next part. The strategy level definitions represent the aim of this proposed challenge (Braking strategy and EMS blocks).

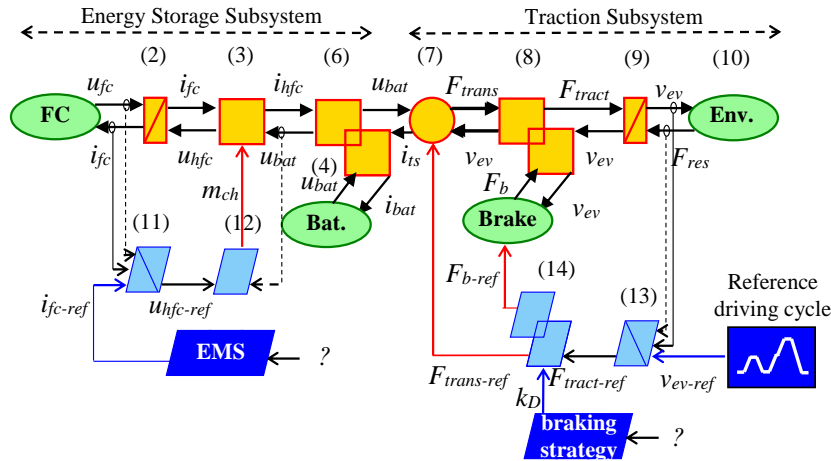


Fig. 6 EMR and inversion-based control of the studied fuel cell vehicle

IV. ENERGY MANAGEMENT STRATEGY DESIGN

A. Specification and Scoring

Depending on the driving cycle, the traction subsystem will impose the traction current i_{ts} to the ESS depending on the developed traction braking strategy, the vehicle characteristics and the corresponding control. The energetic performances of the studied FC/battery vehicle then will depend on the developed energy management strategy. In this way, the participants of this challenge must develop a robust EMS to:

1) **Increase the fuel cell' lifetime.** A FC degradation function Δ_{fc} is considered. It depends on the FC power operation and start/stop cycles following a quadratic function (16) [13] [23]:

$$\Delta_{fc}(t) = \int_0^t \delta(t) dt + N_{switch} \Delta_{switch} \quad (15)$$

$$\delta(t) = \frac{\delta_0}{3600} \left(1 + \frac{\alpha}{P_{fc-nom}^2} (P_{fc}(t) - P_{fc-nom})^2 \right) \quad (16)$$

where N_{switch} is the number of start of the FC, Δ_{switch} a start-

stop degradation coefficient, δ_0 and α are load coefficients and P_{fc-nom} the nominal power of the FC in term of degradation. In this challenge, the FC is considered as ON when its current i_{fc} is higher than 1 mA. No Open Circuit Voltage (OCV) is considered. The degradation function Δ_{fc} is then expressed between 0 (start of life) and 1 (end of life). In this way, commercial FC system for EV have an average lifetime requirement of 5000 h [13]. During a trip, the cost of the FC system degradation $\$_{\Delta_{fc}}$ (in US \$) can then be calculated depending on the degradation function Δ_{fc} and the FC system cost FC_{cost} .

$$\$_{\Delta_{fc}}(t) = \Delta_{fc}(t) FC_{cost} \quad (17)$$

with $FC_{cost}=600$ US \$ based on the 2020' automotive FC system target defined by the US Department of Energy [24].

2) **Minimize the hydrogen consumption.** The hydrogen mass flow is function of the fuel cell current as presented in Fig. 3. b. The H_2 trip cost can be calculated considering the total fuel consumption:

$$\$_{H_2} = \int_0^t \dot{m}_{H_2} dt H_{2-cost} \quad (18)$$

with $H_{2-cost}=3.5$ US \$/kg H_2 based on the 2020' projection [24]

[11].

3) **Limit the batteries SoC.** The battery degradation depends on its SoC and on the power transients. For example, high currents and especially high recharge currents in the battery reduce its lifetime. A battery degradation function $\Delta_{bat} \in [0,1]$ can be calculated as:

$$\Delta_{bat}(t) = \frac{1}{Q_{bat-max}} \int_0^t |F(SoC_{bat})G(i_{bat})i_{bat}(t)| dt \quad (19)$$

$$\text{with } F(SoC_{bat}) = 1 + 3.25(1 - SoC_{bat})^2 \quad (20)$$

$$\begin{cases} G(i_{bat}) = 1 + 0.45 \frac{i_{bat}}{i_{bat-nom}} & \text{if } i_{bat} \geq 0 \\ G(i_{bat}) = 1 + 0.55 \frac{|i_{bat}|}{i_{bat-nom}} & \text{if } i_{bat} < 0 \end{cases} \quad (21)$$

where $Q_{bat-max}$ is the entire life battery capacity and $i_{bat-nom}$ the nominal current related to the battery capacity Q_{bat} . The battery system degradation cost is then calculated from Δ_{bat} and the initial battery cost.

$$\$_{bat}(t) = \Delta_{bat}(t)BAT_{cost} \quad (22)$$

with $BAT_{cost} = 640$ US \$ (200 US \$/kWh in 2020) [25].

In order to develop and test their strategies, participants will be provided with a Matlab Simulink™ simulation tool (see §IV.B). Different driving cycles will be available for this purpose. However, the developed EMS will be scored with an unknown driving cycle including urban and extra urban driving. The aim of the challenge is to propose real-time strategies: the knowledge of the driving cycle is not known beforehand and offline optimization cannot be include into the final strategy blocks.

Depending on the developed EMS, a battery charge penalty will be set up. Note that this recharge step must not be developed by the participants. In this way, the scoring step will automatically full charged the battery at the best FC efficiency point at the end of the scoring driving cycle. The cost of this recharge step penalty $\$_{charge}$ is then taking into account for the global cost function definition $\$_{global}$:

$$\$_{global} = \$_{fc} + \$_{H2} + \$_{bat} + \$_{charge} \quad (23)$$

B. Matlab Simulink Simulation Program

The EMR and the control scheme of the vehicle is implemented in MATLAB-Simulink™, which is chosen as simulation software using EMR Simulink™ library with basic elements [26] (Fig. 7). Four driving cycles are proposed to develop and test the participants' strategies.

- An adapted NEDC (New European Driving Cycle) which is generally used to determined CO₂ emissions, energy consumption or vehicle range (Fig. 8. a). Here, the speed limitation is 85 km/h.
- A class 2 WLTC (Worldwide harmonized Light vehicles Test Procedures). It has been used since 2015 to harmonize the worldwide driving behavior (Fig. 8. b). The class 2 referred to the maximum power and speed of the studied vehicle [27].

- An urban driving cycle from a Tazzari Zero on-road test realized around the University of Lille 1 (Fig. 8. d).

One driver and one passenger are considered in the car. Several global measurements are listed in the Analyze bloc diagram (right part of the Fig. 7). Note that even if the proposed program is an open simulation program, participants cannot modify the system model. All the numerical values of the simulation parameters will be provided as an initialization file. The simulation procedure is defined in a "read me" file from the downloadable Matlab Simulink™ file available on the IEEE VTS'17 challenge website [28].

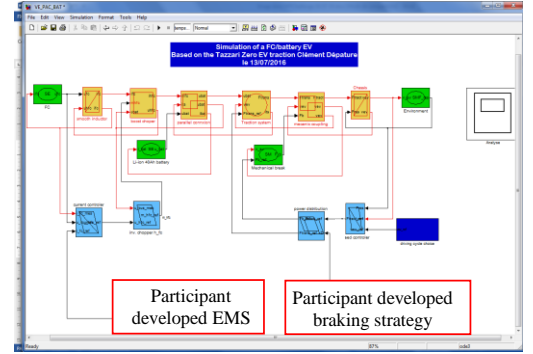


Fig. 7. Matlab Simulink™ Simulation program

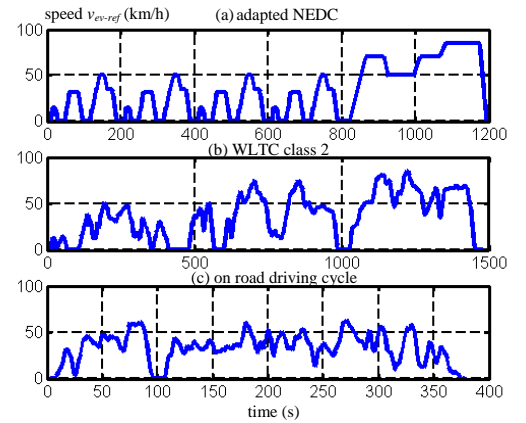


Fig. 8. Considered driving cycle for the EMS development

C. Participation procedure

Participants are invited to respond to this challenge by following the participation procedure describes in the IEEE VTS Challenge website [28]:

<http://www.uqtr.ca/VTSMotorVehiclesChallenge17>

V. CONCLUSION

In order to reach the best performances of the system, the strategy has to manage the electric requirements from the FC (i_{fc-ref}) and the distribution of the braking force between the electric and mechanical brakes (k_D). The aim of this challenge is to design these strategy blocks and to integrate them in the simulation. The objective is to develop a robust Energy Management Strategy to increase energy sources' lifetime

and minimize the hydrogen consumption. In this way, participants shall be ranked on the basis of a cost function which takes into account the FC and battery degradation and the hydrogen consumption. The proposed challenge can then promote the realization of future innovative EMS techniques.

REFERENCES

[1] C.C. Chan, A. Bouscayrol, and K. Chen, "Electric, Hybrid and Fuel Cell Vehicles: Architectures and Modeling", *IEEE Trans. Veh. Tech.*, vol. 59, no. 2, pp. 589 – 598, Feb. 2010.

[2] C. C. Chan, "Overview of Electric, Hybrid and Fuel Cell Vehicles", *Chapter 51, Encyclopedia of Automotive Engineering*, John Willy's & Sons, Ltd, 2015.

[3] M. Zandi, A. Payman, J.-P. Martin, S. Pierfederici, B. Davat, and F. Meibody-Tabar, "Energy Management of a Fuel Cell/Supercapacitor/Battery Power Source for Electric Vehicular Applications", *IEEE Trans. Veh. Tech.*, vol. 60, no. 2, pp. 433–443, Feb. 2011.

[4] F. R. Salmasi, "Control Strategies for Hybrid Electric Vehicles: Evolution, Classification, Comparison, and Future Trends", *IEEE Transactions on Vehicular Technology*, vol. 56, no.5, pp. 2393 – 2404, Sep. 2007.

[5] L. Guzzella, and A. Sciarretta, "Vehicle Propulsion Systems, Introduction to Modelling and Optimization", Second edition, Springer, ISBN 978-3642094156, Oct. 2010.

[6] S. Ahmadi, and S. M. T. Bathaee, "Multi-objective genetic optimization of the fuel cell hybrid vehicle supervisory system: Fuzzy logic and operating mode control strategies," *Int. J. Hydrog. Energy*, vol. 40, no. 36, pp. 12512–12521, Sep. 2015.

[7] K. Ettihir, L. Boulon, and K. Agbossou, "Optimization-based energy management strategy for a fuel cell/battery hybrid power system," *Appl. Energy*, vol. 163, pp. 142–153, Feb. 2016.

[8] A. Castaings, W. Lhomme, R. Trigui, and A. Bouscayrol, "Practical control schemes of a battery/supercapacitor system for electric vehicle", *IET Electrical Systems in Transportation*, vol. 6, no. 1, pp. 20 –26, Mar. 2016.

[9] P. Thounthong, V. Chunkag, P. Sethakul, B. Davat, and M. Hinaje, "Comparative Study of Fuel-Cell Vehicle Hybridization with Battery or Supercapacitor Storage Device", *IEEE Trans. on Veh. Tech.*, vol. 58, no. 8, pp. 3892–3904, Oct. 2009.

[10] <http://www.tazzari-zero.com/> - "Tazzari Zero Website", Apr. 2016.

[11] H. Liu, A. Almansoori, M. Fowler, and A. Elkamel, "Analysis of Ontario's hydrogen economy demands from hydrogen fuel cell vehicles", *Int. Journal of Hydrogen Energy*, vol. 37, no. 11, pp. 8905–8916, Jun. 2012.

[12] V. Liso, M. Pagh Nielsen, and S. Knudsen Koer, "Thermal modeling and temperature control of a PEM fuel cell system for forklift application", *Int. Journal of Hydrogen Energy*, vol. 39, pp. 8410–8420, Apr. 2014.

[13] H. Chen, P. Pei, and M. Song, "Lifetime prediction and the economic lifetime of Proton Exchange Membrane fuel cells", *Applied Energy*, vol. 142, pp. 154–163, Mar. 2015.

[14] J.H. Kim, E. A. Cho, J. H. Jang, H. J. Kim, T. H. Lim, I. H. Oh, J. J. Ko, and S. C. Oh, "Development of a durable PEMFC startup process by applying a dummy load", *Journal of the Electrochemical Society*, vol. 156, no. 8, pp. B995–B961, Jun. 2009.

[15] H. Babazadeh, B. Asghari, and R. Sharma, "A New Control Scheme in a Multi-Battery Management System for Expanding Microgrids", *ISGT'14*, Washington (USA), Feb. 2014.

[16] A. Bouscayrol, B. Davat, B. de Fornel, B. François, J. P. Hautier, F. Meibody-Tabar, E. Monmasson, M. Pietrzak-David, H. Razik, E. Semail, and M.F. Benkhoris, "Control Structures for Multi-machine Multi-converter Systems with upstream coupling," *Math. Compu. Simul.*, vol. 63, no. 3-5, pp. 261–270, Nov. 2003.

[17] A. Bouscayrol, J. P. Hautier, and B. Lemaire Semail, "Systemic design methodologies for electrical energy systems Analysis, Synthesis and Management", Chapter 3: Graphic formalism for the control of multi-physical energetic system: CoG and EMR, *ISTE and Wiley*, ISBN 978-1-84821-3888-3, 2012.

[18] P. Delarue, A. Bouscayrol, and E. Semail, "Generic control method of multi-leg voltage-source-converters for fast practical implementation", *IEEE Trans. Power Elec.*, vol. 18, no. 2, pp. 517–526, Mar. 2003.

[19] K. Thirugnanam, E. R. J. T. P. M. Singh, and P. Kumar, "Mathematical Modeling of Li-Ion Battery Using Genetic Algorithm Approach for V2G Applications", *IEEE Trans. Ener. Conv.*, vol. 29, no. 2, pp. 332 – 343, Jan. 2014.

[20] C. Dépature, W. Lhomme, A. Bouscayrol, P. Sicard, and L. Boulon, "Efficiency map of the traction system of an electric vehicle from an on-road test drive", *IEEE-VPPC'14*, Coimbra (Portugal), Nov. 2014.

[21] Q. Hu, and G. P. Rangaiah, "Anti-Windup schemes for uncertain nonlinear systems", *IEE Proc. Control Theory Appl.*, Vol. 147, no. 3, May 2000.

[22] S. Tarbouriech, and M. Turner, "Anti-windup design: an overview of some recent advances and open problems", *IET Control Theory & Applications*, vol. 3, no. 1, pp. 1–19, Jan. 2009.

[23] N. Herr, J. M. Nicod, C. Varnier, L. Jardin, and A. Sorrentino, "Decision process to manage useful life of multi-stacks fuel cell systems under service constraint", *FDFC'15*, Toulouse (France), Feb. 2015.

[24] USDRIVE, "Fuel Cell Technical Team Roadmap", *technical document*, Jun. 2013.

[25] B. Nykvist, and M. Nilsson, "Rapidly falling cost of battery packs for electric vehicles", *Nat. Climate Change*, vol. 5, pp 329–332, Mar. 2015.

[26] EMR website, <http://www.emrwebsite.org>

[27] M. Tutuianu, A. Marotta, H. Steven, Eva Ericsson, T. Haniu, N. Ichikawa, and H. Ishii, "Development of a World-wide Worldwide harmonized Light duty driving Test Cycle (WLTC)", *Draft Technical Report, DHC subgroup, GRPE-67-03*, Nov. 2013.

[28] <http://www.uqtr.ca/VTSMotorVehiclesChallenge17>

APPENDIX: EMR PICTOGRAMS

	Energy source (ex. battery)		Energy accumulation (ex. inertia)		Closed loop control
	Mono-domain converter (ex. gearbox)		Multi-domain converter (ex. pump)		Open loop control
	Energy distribution (same domain)		Energy distribution (several domain)		Coupling inversion with distribution criteria
	Action – Reaction variables		Sensor		Global energy management